Quantum spiral bandwidth of entangled two-photon states

J. P. Torres, A. Alexandrescu, and Lluis Torner

ICFO–Institut de Ciencies Fotoniques, and Department of Signal Theory and Communications,
Universitat Politecnica de Catalunya, 08034 Barcelona, Spain
(Received 13 June 2003; published 19 November 2003)

We put forward the concept of quantum spiral bandwidth of the spatial mode function of the two-photon entangled state generated in spontaneous parametric down-conversion. We obtain the bandwidth using the eigenstates of the orbital angular momentum of the biphoton states, and reveal its dependence with the length of the down-converting crystals and waist of the pump beam. The connection between the quantum spiral bandwidth and the entropy of entanglement of the quantum state is discussed.

Entanglement, one of the most genuine features of quantum mechanics, is a basic ingredient in quantum cryptography, computing, and teleportation [1,2]. Spontaneous parametric down-conversion, namely, the generation of two lower-frequency photons when a strong pump field interacts with a nonlinear crystal, is a reliable source of entangled photons. The generated two-photon state is entangled in polarization [3], and most applications of parametric down-conversion in quantum systems make use of such spin entanglement [4–6]. However, entanglement is also embedded in the spatial mode functions that describe the two-photon states. Such spatial entanglement occurs in an infinite-dimensional Hilbert space and is gaining increasing attention as a powerful way to encode and to exploit quantum information [7–12]. For example, knowledge of the spatial structure acquired by the mode functions of entangled signal and idler photons forms the basis of multidimensional quantum imaging, and it can be used to increase the efficiency of multidimensional quantum communication protocols. The spatial structure of the photon states can be expressed by a mode decomposition of their mode function in an appropriate basis. The amount of entanglement of a quantum state is directly related to the width of such modal expansion, hereafter referred to as *quantum spatial bandwidth*. A two-photon state described by a single mode is a product state, while a quantum state described by an equidistributed multimode expansion corresponds to a maximally entangled state. Therefore, a fundamental question that arises is how to act on the spatial quantum distribution of a given mode expansion, hence how the corresponding quantum information can be, e.g., *concentrated*. Along these lines, the spatial manipulation of the pump beam have been shown to result in significant alterations of the coincidence counting rate as a function of the transverse spatial coordinates in quantum imaging [7,13,14], which is a signature of the underlying modification of the quantum spatial bandwidth.

It has been recently observed experimentally that the photon pairs generated in spontaneous down-conversion are entangled in orbital angular momentum (OAM) [15]. Such OAM entanglement allows the implementation of arbitrary *d*-dimensional quantum channels [16], thus it has been used to demonstrate violation of Bell inequalities with qutrits [17]. The corresponding mode functions are naturally expressed in terms of eigenstates of the paraxial OAM operator, whose spiral or winding topological structure can be resolved experimentally using combinations of holographic and filtering techniques. Therefore, such base provides a powerful tool to explore the concept of spatial multimode entanglement. In this paper we put forward the full characterization of the entangled photon pairs in terms of eigenstates of the OAM operator and reveal how the corresponding *quantum spiral bandwidth* depends on the shape of the beam that pumps the down-converting crystal, and on the material properties and length of the crystal. We obtain in analytical form important similarity rules that hold for arbitrary input and crystal conditions.

Let a quadratic nonlinear crystal of length L be illuminated by a quasimonochromatic laser pump beam propagating in the z direction. The pump beam writes $E_p(x,z,t) = \int dq E_0(q)\exp[i(k_p(q)z + iq \cdot x - \omega_p t)] + \text{c.c.}$, where ω_p is the angular frequency of the pump beam, $k_p(q) = [(\omega_p n_p/c)^2 - q^2]^{1/2}$ is the longitudinal component of the wave vector, n_p is the refractive index at the pump wavelength, q is the transverse component of the wave vector, x is the position in the transverse plane, and E_0 is the transverse spatial frequency field profile. The signal and idler photons are assumed to be monochromatic, with $\omega_p = \omega_s + \omega_i$, where and ω_s and ω_i are the frequency of the signal and idler photons, respectively. This is justified by the use of narrow-band interference filters in front of the detectors.

In the paraxial approximation, the spin and the OAM can be considered separately [18]. Under these conditions, photons described by a mode function that is a Laguerre-Gaussian (u_p^l) mode are eigenstates of the OAM operator with eigenvalue $l\hbar$ [19]. The index p is the number of non-axial radial nodes of the mode and the index l, referred to as the topological winding number, describes the helical structure of the wave front around a wave front singularity or dislocation. State vectors which are represented by a superposition of LG modes correspond to photons in a superposition state, with the weights of the quantum superposition dictated by the contribution of the lth angular harmonics. When the pump beam is a $u_{p_0}^{l_0}$ mode, under conditions of collinear phase matching, the two-photon state at the output of the nonlinear crystal can be written as a coherent superposition of eigenstates of the OAM operator [20] that are correlated in OAM, i.e., $l_1 + l_2 = l_0$, where l_1 and l_2 refer to the OAM eigenvalues for the signal and idler photons. A photon state described by a LG mode can be written as

$$|lp\rangle = \int dq u_p^l(q) a^\dagger(q)|0\rangle, \tag{1}$$

where the mode function in the spatial frequency domain at $z=0$ is written as

$$u_p^l(\rho,\varphi) = \left(\frac{w_0^2 p!}{2\pi(|l|+p)!}\right)^{1/2} \left(\frac{w_0\rho_k}{\sqrt{2}}\right)^{|l|} L_p^{|l|}\left(\frac{\rho_k^2 w_0^2}{2}\right)$$

$$\times \exp\left(-\frac{\rho_k^2 w_0^2}{4}\right)\exp\left\{il\varphi_k + i\left(p-\frac{|l|}{2}\right)\pi\right\}, \tag{2}$$

with ρ_k and φ_k being the modulus and phase, respectively, of the transverse components q of the wave vector. The functions $L_p^l(\rho)$ are the associated Laguerre polynomials and w_0 is the beamwidth.

The quantum state of the generated two-photon pair is given [21] by

$$|\Psi\rangle = \int dq_s dq_i \Phi(q_s,q_i) a_s^\dagger(q_s) a_i^\dagger(q_i)|0,0\rangle, \tag{3}$$

where $q_{s,i}$ are the transverse components of the signal and idler wave vectors, $|0,0\rangle$ is the vacuum state, and $a_s^\dagger$ and $a_i^\dagger$ are creation operators for the signal and idler modes. Under conditions of collinear propagation of the pump, signal and idler photons, the mode function $\Phi(q_s,q_i)$ can be written as $\Phi(q_s,q_i) = E_0(q_s+q_i)W(q_s-q_i)$, where normalization of the state requires $\int dq_s dq_i |\Phi(q_s,q_i)|^2 = 1$. The function W, which comes from the phase-matching condition in the longitudinal direction, is given [21] by

$$W(q_s,q_i) = \sqrt{\frac{2L}{\pi^2 k_p}}\mathrm{sinc}\left(\frac{|q_s-q_i|^2 L}{4k_p}\right)\exp\left(-i\frac{|q_s-q_i|^2 L}{4k_p}\right), \tag{4}$$

where one makes use of the paraxial approximation $k_p(q) \sim k_p - q^2/(2k_p)$, with $k_p = \omega_p n_p/c$, and correspondingly for the signal and idler wave vectors. The condition $n_p \cong n_s \cong n_s$, where $n_{s,i}$ are the refractive index at the signal and idler wavelengths, is assumed.

One can decompose the quantum state $|\Psi\rangle$ in the base of the eigenstates of the OAM operator, as

$$|\Psi\rangle = \sum_{l_1,p_1}\sum_{l_2,p_2} C_{p_1,p_2}^{l_1,l_2}|l_1,p_1;l_2,p_2\rangle, \tag{5}$$

where (l_1,p_1) correspond to the signal mode, (l_2,p_2) correspond to the idler mode, and the amplitude $C_{p_1,p_2}^{l_1,l_2}$ is written as

$$C_{p_1,p_2}^{l_1,l_2} = \int dq_s dq_i \Phi(q_s,q_i)[u_{p_1}^{l_1}(q_s)]^*[u_{p_2}^{l_2}(q_i)]^*. \tag{6}$$

The weights of the quantum superposition are given by $P_{p_1,p_2}^{l_1,l_2} = |C_{p_1,p_2}^{l_1,l_2}|^2$, which gives the value of the joint detection probability for finding one photon in the signal mode (l_1,p_1) and one photon in the idler mode (l_2,p_2). The two-photon state can be also characterized by the amplitude $A(x_1,z_1,t_1;x_2,z_2,t_2) = \langle 0,0|E_1^+ E_2^+|\Psi\rangle$, at positions (x_1,z_1) and (x_2,z_2) and times t_1 and t_2, where $E^+(x,z,t)$ is the
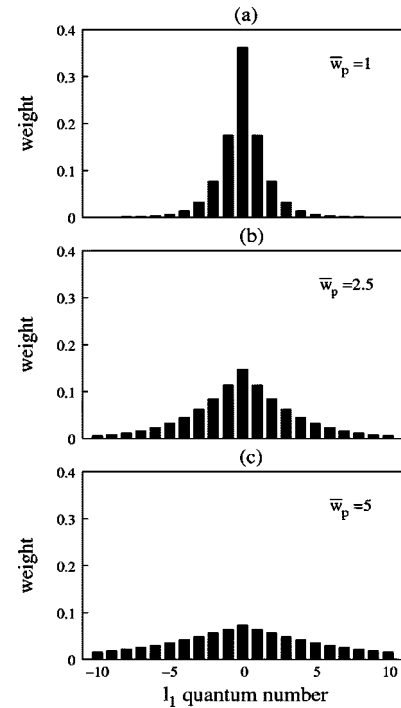

FIG. 1. Mode distributions P_{l_1,l_2} for different values of the parameter $\bar{w}_p$, which takes into account all the harmonics with the same indices l_1 and l_2. (a) $\bar{w}_p=1$, (b) $\bar{w}_p=2.5$, and (c) $\bar{w}_p=5$. The pump beam is a Gaussian mode ($l_0=0$), so that $l_1+l_2=0$. The x axis represents the value of l_1.

electric-field operator. If one makes use of the paraxial approximation for the electric-field operator of a photon traveling in vacuum [21,22], the amplitude can be written as

$$A(x_1,z_1,t_1;x_2,z_2,t_2) = \sum_{l_1,p_1}\sum_{l_2,p_2} C_{p_1,p_2}^{l_1,l_2} u_{p_1}^{l_1}(x_1,z_1) u_{p_2}^{l_2}(x_2,z_2)$$

$$\times \exp[-i\omega(t_1+t_2)]. \tag{7}$$

Such amplitude might be employed, e.g., to draw analogies between the spatial structure of the two-photon quantum states and the properties of the corresponding incoherent classical radiation (see Refs. [11,21]).

For a given nonlinear crystal and pump beam spatial distribution, the amplitudes $C_{p_1,p_2}^{l_1,l_2}$ depend on the length of the crystal (L), the pump beam width w_p, and the chosen width of the LG base (w_0). Through the normalization of Eq. (6), it turns out that the amplitude can be shown to depend on two normalized parameters: the normalized pump beam width $\bar{w}_p = w_p/\sqrt{\lambda_p L}$ and the normalized beam width of the LG modes, $\bar{w}_0 = w_0/\sqrt{\lambda_p L}$, where λ_p is the wavelength of the pump beam in vacuum. For a typical value of the pump wavelength $\lambda_p = 0.4$ μm, and a crystal length of $L=1$ mm, a pump beam width of $w_p \sim 20$ μm corresponds to a normalized value of $\bar{w}_p \sim 1$.

In Fig. 1 we plot the contribution to the mode decomposition of the quantum state $|\Psi\rangle$ of all the harmonics with the same value of the indices l_1 and l_2, i.e., $P_{l_1,l_2} = \sum_{p_1,p_2=0}^\infty P_{p_1,p_2}^{l_1,l_2}$, which gives the probability of detecting a
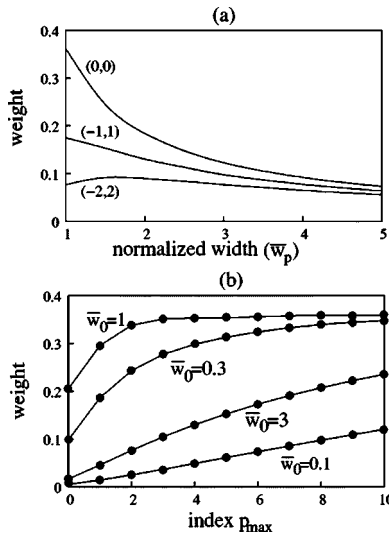
FIG. 2. (a) Value of the weight P_{l_1,l_2} for $(l_1,l_2)=(0,0)$, $(1,-1)$, and $(2,-2)$, as a function of the normalized pump beam width $\bar{w}_p$. The labels show the value of (l_1,l_2). The pump beam is a Gaussian mode. (b) Weight $P^{0,0}_{p_{max}}$ as a function of the index p_{max} for different values of $\bar{w}_0$, as shown in the labels. In all cases $\bar{w}_p=1$.

photon with signal mode l_1 and idler mode l_2, for any value of p_1 and p_2. In all cases the pump beam is a Gaussian mode. The distribution P_{l_1,l_2} depends only on the normalized width $\bar{w}_p$. Thus, for a given material, the OAM distribution of the state $|\Psi\rangle$ depends on the ratio $w_p/\sqrt{\lambda_p L}$, a result which gives an important scaling rule. In Fig. 2(a) we show the dependence of P_{l_1,l_2} on $\bar{w}_p$ for different values of l_1 and l_2, with $l_1+l_2=0$. One observes that the spiral bandwidth increases with $\bar{w}_p$, therefore it can be made larger by increasing the pump beam width or by decreasing the crystal length. Notice that in doing so the coupling efficiency in the detection state is also modified (see, e.g., Ref. [23]). Although the total contribution P_{l_1,l_2} of modes with a given index l_1 and l_2 depends only on $\bar{w}_p$, the actual amplitude distribution $P^{l_1,l_2}_{p_1,p_2}$ depends also on $\bar{w}_0$. In Fig. 2(b) we show the contributions of the modes with different indices p_1 and p_2, i.e., $P^{0,0}_{p_{max}}=\Sigma^{p_{max}}_{p_1,p_2=0}P^{l_1,l_2}_{p_1,p_2}$, as a function of p_{max}. We consider $\bar{w}_p=1$ and $l_1=l_2=0$, which is representative of a general case. The plot reveals that there is an optimal value of $\bar{w}_0$ for which the contribution of $P^{0,0}_{0,0}$ is maximum, and only a few modes with different index p make significant contributions to the total weight. Away from the optimal $\bar{w}_0$ value, a large number of modes are required to represent the quantum state.

In most applications that make use of the OAM of the photons, one projects into a subspace of the complete Hilbert space that describes the mode function of the photon (e.g., Ref. [17]). This implies considering only a fraction of the mode space. Let us consider only modes with $p_1=p_2=0$, and thus thereafter we define $|l_1,l_2\rangle\equiv|l_1,p_1=0;l_2,p_2=0\rangle$. In this subspace, the two-photon state can be written as

$$|\Psi\rangle=\sum_{l_1=-\infty}^{\infty}\sum_{l_2=-\infty}^{\infty}C_{0,0}^{l_1,l_2}|l_1,l_2\rangle. \tag{8}$$

Since the amplitude $C_{0,0}^{l_1,l_2}$ depends on both normalized parameters $\bar{w}_p$ and $\bar{w}_0$, the expansion given by Eq. (8) depends on the base of LG modes considered. In general, calculation of the amplitudes $C_{p_1,p_2}^{l_1,l_2}$ requires a four-dimensional integration in the spatial frequency domain. However, for a pump beam with a spatial field profile corresponding to a $u_0^{l_0}$ mode, we were able to obtain the value of the amplitude $C_{0,0}^{l_1,l_2}$ in an analytic form. Namely,

$$C_{0,0}^{l_1,l_2}=A_0\Gamma\left(\frac{|l_0|+|l_1|+|l_2|}{2}+1\right)\tan^{-1}\frac{1}{i+w_0^2k_p/2L} \tag{9}$$

for $l_1l_2\geq0$, and

$$C_{0,0}^{l_1,l_2}=A_0\sum_{n=0}^{\min(|l_1|,|l_2|)}(-1)^n\frac{|l_1|!|l_2|!}{(|l_1|-n)!(|l_2|-n)!(n!)^2}$$

$$\times\left(\frac{w_0^2}{2w_p^2+w_0^2}\right)^{-n}\frac{\Gamma\left(\frac{|l_0|+|l_1|+|l_2|-2n}{2}+1\right)}{(1+i(4L/w_0^2k_p))^{n/2}}$$

$$\times\Gamma(n)\sin\left(n\tan^{-1}\frac{1}{i+w_0^2k_p/2L}\right) \tag{10}$$

for $l_1l_2<0$. In these expressions, A_0 stands for

$$A_0=(-i)^{|l_0|-|l_1|-|l_2|}(k_pw_p^2/\pi L)^{1/2}(w_p/w_0)^{|l_p|}$$

$$\times\left(\frac{2w_0^2}{2w_p^2+w_0^2}\right)^{(|l_0|+|l_1|+|l_2|)/2+1}\frac{2^{(|l_0|-|l_1|-|l_2|)/2+1}}{\sqrt{|l_0|!|l_1|!|l_2|!}}. \tag{11}$$

In both Eqs. (9) and (10), the relation $l_0=l_1+l_2$ holds. It is worth stressing that Eqs. (9)–(11) provide the analytical expression of the quantum state under general conditions in terms of the pump beam and the crystal properties. Moreover, this expansion corresponds to performing a Schmidt decomposition for continuous variables in this subspace, thus allowing to calculate the entropy of entanglement [24].

In Fig. 3, we plot the expansion in OAM eigenstates of the two-photon state for pump beams with $l_0=0,1,2$ and $\bar{w}_p=\bar{w}_0=1$. In the three cases represented, the subspace we are considering represents more than 40% of the corresponding complete Hilbert space. The spiral bandwidth of the expansion in terms of states $|l_1,l_2\rangle$ increases with l_0. Equations (9) and (10) show that, for a given pump beam, the phase of the amplitude $C_{0,0}^{l_1,l_2}$ changes for each mode with $l_1l_2<0$, but it is the same for all modes with $l_1l_2\geq0$.

The concept can be extended to the general case of a pump beam whose spatial field distribution is a coherent superposition of LG modes, so that $E_0(x)=\Sigma_m C_m u_0^m(x)$, with $m=0,2,4,\ldots,M$. The LG modes $u_0^m(x)$ are the corresponding expression in the spatial domain of the LG modes given
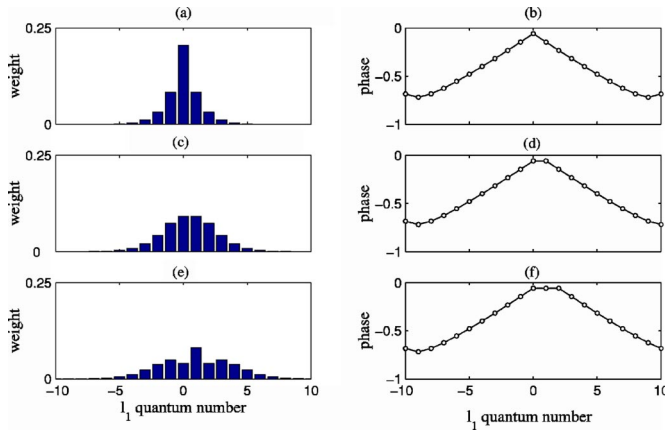
FIG. 3. Mode decomposition in the subspace $|l_1,p_1=0;l_2,p_2=0\rangle$ for several pump beams. In (a), (c), and (e) we plot the weight $P_{0,0}^{l_1,l_2}$ of the mode distribution, and in (b), (d), and (f) we plot the phase $\arg\{C_{0,0}^{l_1,l_2}\}$ of each mode. (a,b): $l_0=0$; (c,d): $l_0=1$ and (e,f): $l_0=2$. In all cases, $\bar{w}_p=\bar{w}_0=1$. The solid line in (b–d) is plotted to help the eye.

by Eq. (2). The energy flow I of the pump beam can be written as [16] $I=2\epsilon_0 c n_p\Sigma_m|C_m|^2$. If we restrict to the subspace spanned by the states of the form $|l,l\rangle$, one generates an entangled two-photon state of the form $|\Psi\rangle\sim\Sigma_{n=0}^N\gamma_n|n,n\rangle$. By making use of Eqs. (9) and (10), one obtains that the amplitudes γ_n of the quantum state generated when the crystal is pumped by the superposition of LG modes are

$$\gamma_n=\frac{\sqrt{(2n)!}}{n!}\{2\bar{w}_p/[\bar{w}_0(2\bar{w}_p^2+1)]\}^{2n+2}C_{2n}. \quad (12)$$

This expression reveals that properly tailoring the spatial features of the beam that pumps the down-converting crystal allows generation of optimal quantum states for different quantum information protocols, such as the entanglement enhancement required for obtaining maximally entangled states [25]. One approach for the realization of entanglement concentration is to perform mode filtering operations on the two-photon state that is generated at the output of the crystal [26]. In contrast, Eq. (12) shows that the required quantum state could be obtained through appropriate engineering of the spatial properties of the pump beam [27]. For instance, Eq. (12) gives the contribution C_{2n} of each mode that makes the pump beam, in order to obtain a maximally entangled quantum state ($\gamma_n=1$, all n). Equation (12) also shows that the phase of the state $|n,n\rangle$ corresponds to the phase of the corresponding mode of the classical pump beam, $\arg\{C_{2n}\}$, a result consistent with the experimental observation by Ou *et al.*, that the down-converted photons carry information about the phase of the pump beam [28].

In conclusion, we have obtained and analyzed the detailed quantum spatial structure of the two-photon entangled states generated in parametric down-conversion in terms of the eigenstates of the orbital angular momentum operator. We put forward the related concept of quantum spiral bandwidth, and showed its dependence on the pump beam and down-converting crystal. This allows us, e.g., to define an effective finite Hilbert space where entanglement takes place [29]. Engineering such quantum spatial bandwidth should be a key tool to optimize multidimensional quantum information schemes, for example, to increase the resolution of two-photon imaging using entangled photons (e.g., Ref. [30]) and to enhance the efficiency of relevant multidimensional quantum cryptography protocols (e.g., Ref. [31]).

[1] M.A. Nielsen and I.L. Chaung, *Quantum Computation and Quantum Information* (Cambridge University Press, Cambridge, 2000).
[2] *The Physics of Quantum Information*, edited by D. Bouwmeester *et al.* (Springer, Berlin, 2000).
[3] P.G. Kwiat *et al.*, Phys. Rev. Lett. **75**, 4337 (1995).
[4] D. Bouwmeester *et al.*, Nature (London) **390**, 575 (1997).
[5] D. Bouwmeester *et al.*, Phys. Rev. Lett. **82**, 1345 (1999).
[6] T. Jennewein *et al.* Phys. Rev. Lett. **84**, 4729 (2000).
[7] T.B. Pittman *et al.*, Phys. Rev. A **53**, 2804 (1996).
[8] K. Banaszek *et al.*, Opt. Lett. **26**, 1367 (2001).
[9] C. Simon and J.W. Pan, Phys. Rev. Lett. **89**, 257901 (2002).
[10] P. Navez *et al.*, Phys. Rev. A **65**, 013813 (2002).
[11] A. Gatti *et al.*, Phys. Rev. Lett. **90**, 133603 (2003).
[12] A.M. Dawes *et al.*, Phys. Rev. A **67**, 032102 (2003).
[13] D.V. Strekalov *et al.*, Phys. Rev. Lett. **74**, 3600 (1995).
[14] C.H. Monken *et al.*, Phys. Rev. A **57**, 3123 (1998).
[15] A. Mair *et al.*, Nature (London) **412**, 313 (2001).
[16] G. Molina-Terriza *et al.*, Phys. Rev. Lett. **88**, 013601 (2002).

[17] A. Vaziri *et al.*, Phys. Rev. Lett. **89**, 240401 (2002).
[18] S.M. Barnett, J. Opt. B: Quantum Semiclassical Opt. **4**, S7 (2002).
[19] L. Allen *et al.*, in *Progress in Optics*, edited by E. Wolf (Elsevier, Amsterdam, 1999), Vol. XXXIX, pp. 291–372.
[20] S. Franke-Arnold *et al.*, Phys. Rev. A **65**, 033823 (2002).
[21] B.E.A. Saleh *et al.*, Phys. Rev. A **62**, 043816 (2000).
[22] S.P. Walborn *et al.*, Phys. Rev. Lett. **90**, 143601 (2003).
[23] F.A. Bovino *et al.*, e-print quant-ph/03003126.
[24] S. Parker *et al.*, Phys. Rev. A **61**, 032305 (2000)
[25] C.H. Bennett *et al.*, Phys. Rev. A **53**, 2046 (1996).
[26] A. Vaziri *et al.*, e-print quant-ph/0303003.
[27] J.P. Torres *et al.*, Phys. Rev. A **67**, 052313 (2003).
[28] Z.Y. Ou *et al.*, Phys. Rev. A **41**, 566 (1990).
[29] C.K. Law *et al.*, Phys. Rev. Lett. **84**, 5304 (2000).
[30] A.F. Abouraddy *et al.*, J. Opt. Soc. Am. B **19**, 1174 (2002).
[31] H. Bechmann-Pasquinucci and A. Peres, Phys. Rev. Lett. **85**, 3313 (2000); Č. Brukner *et al.*, *ibid.* **89**, 197901 (2002).